Macromolecules
ARTICLE

Macromolecules **2010**, *43*, 1771–1777 **1771**
DOI: 10.1021/ma902590w

Thermoresponsive Core−Shell Brush Copolymers with Poly(propylene oxide)-*block*-poly(ethylene oxide) Side Chains via a "Grafting from" Technique

Junpeng Zhao,[†,‡] Grigoris Mountrichas,[‡] Guangzhao Zhang,[†] and Stergios Pispas*[,‡]

[†]*Hefei National Laboratory for Physical Sciences at Microscale, University of Science and Technology of China, Hefei 230026, Anhui, China, and* [‡]*Theoretical and Physical Chemistry Institute, National Hellenic Research Foundation, 48 Vass. Constantinou Ave., 11635 Athens, Greece*

Received November 24, 2009; Revised Manuscript Received January 14, 2010

ABSTRACT: Thermoresponsive brush copolymers with poly(propylene oxide)-*block*-poly(ethylene oxide) side chains were synthesized via a "grafting from" technique. Near-monodisperse poly(*p*-hydroxystyrene) was used as the backbone, and the brush copolymers were prepared by sequential metal-free anionic ring-opening polymerization of the oxyalkylene monomers, using the phosphazene base (*t*-BuP_4) and the phenolic hydroxyl groups in the backbone to generate the complex multifunctional initiating system. The length and composition of the side chains were varied by changing the feed ratios of the backbone and the side-chain monomers. By inverting the sequence of the monomer addition, two different molecular structures were achieved, with either poly(propylene oxide) or poly(ethylene oxide) linked to the backbone. In all cases, brush copolymers with high molecular weights and low molecular weight distributions were synthesized. The thermoresponsive behavior of the brush copolymers in dilute aqueous solutions was investigated by dynamic/static light scattering and fluorescence measurements. Temperature-induced intramolecular chain contraction/association and intermolecular aggregation could both be observed at different stages of the heating process. Intermolecular aggregation was more pronounced for the sample with the poly(propylene oxide) blocks located at the periphery. The results from fluorescence spectroscopy indicate the incompletely solvated state of the brush copolymer in aqueous solution at low temperature and the absence of compact hydrophobic domains in some of the aggregates due to the core−shell brushlike molecular structure of the copolymers.

Introduction

Graft copolymers with densely grafted side chains (or brush copolymers) have gained significant academic interest due to their inherent properties related to the multibranched molecular structures, such as the extended chain conformations resulting from the intramolecular excluded-volume interactions among the densely grafted side chains.[1,2] Of all brush copolymers, those consisting of diblock copolymer side chains have attracted increasing attention in recent years due to their unique core−shell nanoscopic molecular structures and their potential application in preparing core−shell nanomaterials.[1,3−14]

Attempts have been made to develop new synthetic methods aiming at (i) varying the nature of the backbones and the side chains and (ii) controlling the chain length and composition of the side chains.[3−12] Two synthetic methodologies for the creation of core−shell brush copolymers can be found in the literature: (i) the polymerization of diblock macromonomers ("grafting through" approach)[3−6] and (ii) the sequential polymerization of two different monomers initiated by multifunctional macroinitiators ("grafting from" approach).[7−12] Because of the inherent disadvantages lying in the "grafting through" technique (poor molecular weight control, incomplete conversion of the macromonomer, broad molecular weight distribution),[1] the "grafting from" technique seems to be more preferable for the preparation of core−shell brush copolymers. So far, the polymerization methods employed for the creation of the diblock side chains are living radical polymerizations, including atom transfer radical polymerization,[7−9] nitroxide-mediated polymerization,[10,11] and reversible addition−fragmentation chain transfer polymerization.[12] Ionic polymerizations have not been used extensively, even for the preparation of graft copolymers with homopolymer side chains,[15,16] because of the difficulties associated with the preparation of polyionic macroinitiators.

Block copolymers based on poly(propylene oxide) (PPO) and poly(ethylene oxide) (PEO) have been studied extensively as a family of amphiphilic block copolymers assembling into polymeric micelles at elevated temperatures.[17−19] The molecular structure has been found to be one of the fundamental parameters (others being temperature, molecular composition, additive, etc.) that affect the micellization behavior of these poly(oxyalkylene)-based copolymers. Up to present, the molecular structures studied include diblock, triblock (PEO-*b*-PPO-*b*-PEO and PPO-*b*-PEO-*b*-PPO), and cyclic copolymers.[18] Graft copolymers containing both PEO and PPO have been reported scarcely regarding both their synthesis and physical properties.[3,20,21]

The phosphazene base *t*-BuP_4, has been used to generate effective counterions, either with lithium cation ($[t\text{-Bu}P_4\text{Li}]^+$)[22−24] or with proton ($[t\text{-Bu}P_4\text{H}]^+$),[25−29] for the anionic polymerization of oxyalkylenes. However, the synthesis of block copolymers via sequential addition of different oxyalkylene monomers in the presence of *t*-BuP_4 has been reported in only one case.[24]

In this paper, we report on the synthesis of core−shell brush copolymers with PPO-*b*-PEO side chains, using $[t\text{-Bu}P_4\text{H}]^+$ as the counterion, via anionic polymerization high-vacuum techniques. Poly(*p*-hydroxystyrene) (PHOS) with narrow molecular weight distribution was utilized as the backbone polymer to

*Corresponding author: Tel +30210-7273824; Fax +30210-7273794; e-mail pispas@eie.gr.

Published on Web 01/25/2010

Scheme 1. General Synthetic Scheme for the Preparation of the Core−Shell Brush Copolymers

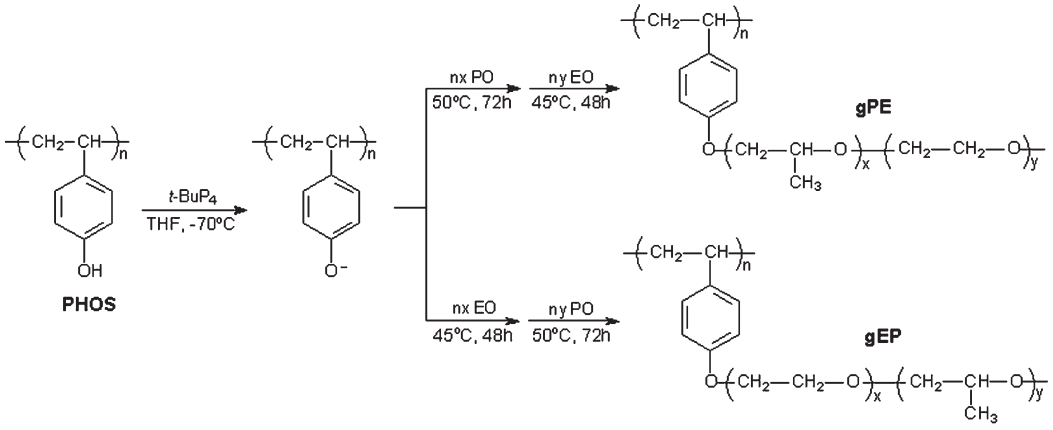

Table 1. Molecular Characteristics of the Core−Shell Brush Copolymers

sample	$M_{arm,theo}$[b] × 10^{-4} (g/mol)	$f_{PO,theo}$[c] (%)	$M_{w,SEC}$[d] × 10^{-5} (g/mol)	M_w/M_n[d]	f_g[e] (%)	$M_{w,cal}$[f] × 10^{-5} (g/mol)	$M_{w,LS}$[g] × 10^{-5} (g/mol)	$M_{w,arm}$[h] × 10^{-4} (g/mol)	f_{PO}[i] (%)
gPE1[a]	2.22	33.3	5.65	1.15	52.4	11.15	15.25	1.75	32.5
gPE2	2.26	52.4	4.15	1.14	40.1	8.19	11.35	1.30	59.2
gPE3	1.22	71.4	2.58	1.08	55.5	5.94	7.46	0.74	76.6
gEP1	2.15	37.3	4.98	1.15	58.2	10.94	14.21	1.63	15.1

[a] Poly(*p*-hydroxystyrene)-*g*-[poly(propylene oxide)-*b*-poly(ethylene oxide)] and poly(*p*-hydroxystyrene)-*g*-[poly(ethylene oxide)-*b*-poly(propylene oxide)] are termed as gPE and gEP, respectively. [b] Theoretical molecular weight of the side chain calculated by the feed ratio of the monomers to the backbone. [c] Theoretical weight fraction of PO calculated by the feed ratio of the two monomers. [d] By SEC. [e] Weight fraction of the core−shell brush copolymer in the crude product (from SEC analysis). [f] Calculated by f_g and the known molecular weight of the backbone. [g] Obtained from Zimm plots for the brush copolymer in its aqueous solutions at low temperature (25 °C). [h] Molecular weight of each side chain calculated by $M_{w,LS}$ and the molecular weight of the backbone. [i] Weight fraction of PPO in the fractionated brush copolymer determined by the data of ^{1}H NMR.

generate multifunctional macroinitiators with *t*-BuP_4. The feed ratios of the backbone and side chain monomers were varied in order to acquire different molecular compositions. Moreover, two different sequences of the monomer addition were conducted in order to achieve the two correspondingly inverse molecular topologies in regard to the side chains. The thermoresponsive behavior of the well-defined core−shell brush copolymers in dilute aqueous solutions will also be discussed.

Experimental Section

Polymer Synthesis. All reagents were purchased from Aldrich and purified by well-established procedures for anionic polymerization high-vacuum techniques.[29,30] Tetrahydrofuran (THF) was dried over CaH_2 and then distilled in a flask containing Na/K alloy, where it was stirred and degassed until the color turned to bright blue. Ethylene oxide (EO) and propylene oxide (PO) were respectively stirred sequentially with CaH_2 and *n*-butyllithium (twice), before distillation into graduated ampules. The phosphazene base, *t*-BuP_4, was received from Aldrich in its solution in *n*-hexane. The solvent was removed by distillation, and the solid *t*-BuP_4 was left under high vacuum overnight before dissolved again in purified benzene to the desired concentration.

The synthesis procedure of PHOS, via conventional anionic polymerization of *p-tert*-butoxystyrene and postpolymerization hydrolysis, has been described before.[31,32] The PHOS sample used as the backbone in the present work had the weight-average molecular weight (M_w) of 10 500 g/mol and the molecular weight distribution (M_w/M_n) of 1.18. Before each polymerization, the appropriate amount of the PHOS sample was purified by azeotropic distillation with THF, left under high vacuum for 24 h, and finally dissolved again in dry THF by the aid of cryo-distillation. In order to get a better understanding of the polymerization for the core−shell brush copolymers, the brush copolymers comprised of homopolymer side chains were first synthesized and designated as gPO and gEO for PHOS-*g*-PPO and PHOS-*g*-PEO, respectively. The synthetic procedure for gPO and gEO is similar to the synthesis of block−graft copolymers with PEO side chains[29] and follows the polymerization scheme shown in Scheme 1 for the core−shell brush copolymers, taking into account that only one oxyalkylene monomer was added.

Core−shell brush copolymers were synthesized via sequential metal-free anionic polymerization of PO and EO in THF in the presence of *t*-BuP_4 using PHOS as the backbone, as illustrated in Scheme 1. The core−shell brush copolymers are termed as gPE, when PO was first polymerized, so that PPO was linked to the backbone, and gEP, when EO was first polymerized and PEO was linked to the backbone. Typically, the polymerization for gPE1 (Table 1) was conducted as follows. Purified solvent (dry THF, ~60 mL) was distilled into the polymerization apparatus. The apparatus was degassed and flame-sealed. A predetermined amount of *t*-BuP_4 solution (1.0×10^{-4} mol/mL in benzene, 3.1 mL) was first added, making the molar ratio of *t*-BuP_4 to the phenolic hydroxyl groups (PhOH) in the backbone equal to ~0.9. Subsequently, temperature was decreased to −70 °C, and the THF solution of PHOS (0.041 g in ~15 mL of THF, 3.4×10^{-4} mol of PhOH) was added via a break-seal, upon which the mixture became somewhat turbid because of the poor solubility of the consequently generated polyanion. This solution was stirred for 10 min at −70 °C before PO (2.5 g, 0.043 mol) was introduced by cryo-distillation. The reaction mixture was stirred at −70 °C for 2 h and then slowly heated to 50 °C. The turbidity disappeared gradually at this temperature, indicating the growth of PPO side chains on the backbone. The reaction mixture was stirred at this temperature for 72 h to ensure complete consumption of PO. Then, temperature was decreased to 10 °C, and the second monomer, EO (5.0 g, 0.114 mol), was added by cryo-distillation. After that, the solution was heated slowly to 45 °C and stirred at this temperature for 48 h. Finally, the polymerization was terminated by degassed methanol (~1 mL) and a few drops of concentrated hydrochloric acid (HCl).

The polymerization for gEP followed the same procedure as for gPE, except that EO was first polymerized, and the reaction temperature and time for each monomer were also inverted accordingly. After each polymerization, the solvent was evaporated in a rotary evaporator. The crude product was dried in vacuum overnight and weighed in order to determine the conversion of the monomers, which approached 100% in all cases. The crude product was purified by at least two fractionations, using chloroform as the solvent and *n*-hexane as the precipitant, in order to remove reaction byproducts, especially the linear polymers. The molecular characteristics of the core−shell brush copolymers are listed in Table 1.

Characterization Methods. Size exclusion chromatography (SEC) and nuclear magnetic resonance (^{1}H NMR) were used to determine the molecular weights, compositions, and polydispersities of the copolymers. SEC determinations were performed on a Waters system equipped with a Waters 1515 pump, a Waters 2414 differential refractive index detector, and three μ-styragel columns with a continuous porosity of 10^2-10^5 Å. THF (with 5% v/v triethylamine) was used as the eluent, and the flow rate was 1.0 mL/min at 30 °C. The system was calibrated using a series of monodisperse linear polystyrene standards with weight-average molecular weights in the range of 2500−2 100 000 g/mol. ^{1}H NMR (300 MHz) spectra were recorded on a Bruker AC 300 instrument, operating at 300 MHz, at 25 °C using chloroform-*d* ($CDCl_3$) as the solvent.

For light scattering (LS) and fluorescence measurements, aqueous solutions of each core−shell brush copolymer was made by directly dissolving a predetermined amount of the sample in water at 4 °C overnight. The solutions at lower concentrations were prepared by successive dilution of the stock solution and kept at 4 °C overnight before the measurements.

Light scattering measurements were conducted on an ALV/CGS-3 compact goniometer system (ALV GmbH, Germany), equipped with a ALV-5000/EPP multi-τ digital correlator with 288 channels and an ALV/LSE-5003 light-scattering electronics unit for stepper motor drive and limit switch control. A JDS Uniphase 22 mW He−Ne laser (λ_0 = 632.8 nm) was used as the light source. The details of LS theory can be found elsewhere.[33] Dynamic light scattering (DLS) experiments were carried out at scattering angles ranging from 20° to 150° to obtain the average hydrodynamic radius and hydrodynamic radius distribution, $f(R_h)$. The apparent diffusion coefficient, D_{app}, was obtained by extrapolation to zero angle, which leads to apparent hydrodynamic radius, $\langle R_h \rangle$, via the Stokes−Einstein equation $R_h = k_B T/6\pi\eta_0 D$, where k_B, T, and η_0 are the Boltzmann constant, the absolute temperature, and the solvent viscosity, respectively. In static light scattering (SLS), the weight-average molar mass (M_w) was obtained from the angular/concentration dependence of the absolute excess time-average scattering intensity, known as Rayleigh ratio, on the basis of the Zimm plot. The refractive index increment, dn/dC, of each brush copolymer was estimated as the weighted average of PPO and PEO,[34] using the compositions determined by ^{1}H NMR and assuming that the value does not change appreciably with temperature. It has to be noted that, because the content of the backbone in each brush copolymer is very low (< 1.5 wt %) and the dn/dC values for PPO and PEO are close, the error coming from these assumptions should be very small. Concentrations in the range $4.0 \times 10^{-4}-1.0 \times 10^{-3}$ g/mL were used. In the step-by-step heating process, each solution was heated from 5 °C, within 2−5 °C intervals, and LS measurements were performed 30 min after the stabilization of temperature, so that equilibrium could be reached. The heating was stopped at 60 °C or earlier in cases where macroscopic phase separation occurred.

For fluorescence spectroscopy measurements, pyrene was added to the copolymer solutions at the concentration of 2.7×10^{-7} M. The concentration of the brush copolymer ranged from 4.0×10^{-4} to 1.0×10^{-3} g/mL. The solutions were then allowed to stay at 4 °C overnight to achieve equilibrium.

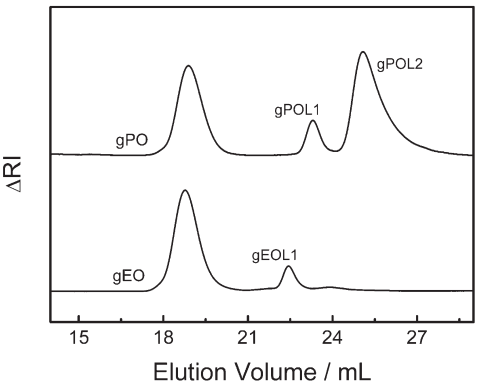

Figure 1. SEC traces for the crude products of the brush copolymers with homopolymer side chains, namely poly(*p*-hydroxystyrene)-*g*-poly(propylene oxide) (gPO) and poly(*p*-hydroxystyrene)-*g*-poly(ethylene oxide) (gEO). Solvent: THF (with 5% v/v triethylamine) at 30 °C and a flow rate of 1 mL/min.

Fluorescence spectra were recorded on a Fluorolog-3, model FL3-21, Jobin Yvon-Spex spectrometer. Excitation wavelength was λ = 335 nm, and emission spectra were recorded in the region 350−500 nm, with an increment of 1 nm, using an integration time of 0.5 s. Slit openings of 1 mm were used for both the excitation and the emitted beams. The I_1/I_3 ratios were determined as the average of three measurements (where I_1 and I_3 are the intensities of the first and the third peaks of the pyrene fluorescence spectra at 372 and 383 nm, respectively). The excimer-to-monomer ratio (I_e/I_m) was calculated as the ratio of the emission intensity at ca. 470 nm to that at 372 nm, respectively. The temperature was controlled using a thermostated cuvette holder connected to a circulating water bath.

Results and Discussion

Synthesis of the Brush Copolymers. The polymerizations for obtaining the brush copolymers with homopolymer side chains, gPO and gEO, were carried out in a manner similar to the procedures followed for the preparation of linear PEO utilizing *t*-BuP_4 as a polymerization promoter,[25−28] in order to validate the experimental graft polymerization conditions for both monomers. Figure 1 gives the SEC traces of gPO and gEO crude products. The peaks located at the lower and higher elution volumes are assigned to the gPO/gEO brush copolymer and linear PPO/PEO byproducts, respectively. For gEO, only one linear PEO peak exists (gEOL1). However, for gPO, two peaks exist at higher elution volumes, indicating that there are two different mechanisms leading to the linear PPO byproducts. It is noticed that the linear polymers with higher molecular weights (gEOL1 and gPOL1) have very low molecular weight distributions (M_w/M_n < 1.05), indicating that the polymerization in these cases also has a controlled character and that the initiating sites exist from the beginning of the polymerization. The impurities, which are brought in with the backbone or *t*-BuP_4 (*t*-BuP_4 is a commercial reagent and was used after minimal purification since it is a solid) and generate initiating sites with *t*-BuP_4, might be the explanation.[29] The second linear PPO byproduct, gPOL2, presents a long tailing in the SEC trace and a much higher polydispersity (M_w/M_n > 1.50). This should be attributed to the chain transfer to PO monomers during the polymerization,[35−39] which generates new initiating sites for linear PPO throughout the polymerization. This chain transfer mechanism inflicts low yield of the gPO brush copolymer. Fortunately, the molecular weight distribution of gPO is not influenced (M_w/M_n = 1.10), which should probably be attributed to the overall protonation−deprotonation equilibrium

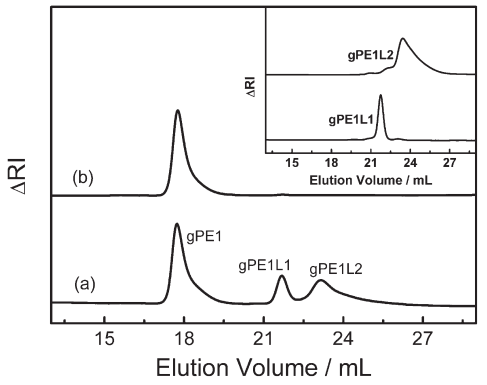

Figure 2. SEC traces of a representative core−shell brush copolymer (gPE1 in Table 1) prepared via metal-free anionic polymerization: (a) crude product before fractionation; (b) pure core−shell brush copolymer after fractionation. Inset: SEC traces of separated linear polymer byproducts after fractionation.

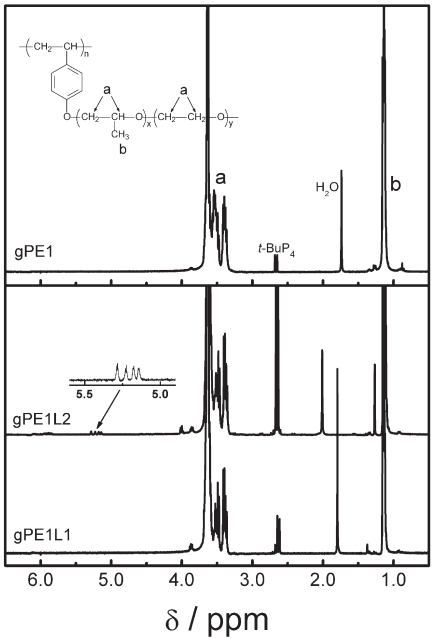

Figure 3. ^{1}H NMR spectra for the three components separated from the crude product of a typical core−shell brush copolymer: gPE1 in Table 1 (upper figure); linear copolymer byproducts, gPE1L1 and gPE1L2 (lower figure).

and/or the brushlike molecular structure. Here we are not going to discuss too much on the brush copolymer with homopolymer side chains, since the graft copolymers with diblock side chains are more desirable.

The core−shell brush copolymers were prepared by sequential polymerization of the two side-chain monomers. Figure 2 gives the SEC traces of a typical gPE product (gPE1) before and after fractionation. Like the case of gPO, two peaks are presented at the higher elution volume in the trace of the crude product, with the first one being symmetric and narrow and the second one having a long tailing. It seems that in this case there are also two mechanisms leading to the linear polymer byproducts, which must be the same as those identified in the case of gPO.

Further fractionations were carefully conducted so as to separate the two linear polymer byproducts (inset of Figure 2). Figure 3 presents the ^{1}H NMR spectra of the three components separated from the crude product of gPE1. All the characteristic peaks of PPO and PEO are clearly present in the spectrum of the brush copolymer. However, the signals of the protons on the backbone are too weak to be seen. The signal coming from *t*-BuP_4 residue can also be observed even after two fractionations. This is because after the termination of the graft polymerization *t*-BuP_4 exists in the protonated state, which is not easy to be removed completely in the fractionation step. It is reported that *t*-BuP_4 residue can be removed completely by ion-exchange resin.[26,28] However, according to our experience, it is possible to introduce some external material (dust and resin fragments) to the final product by using an ion-exchange resin, which would be difficult to be removed completely by standard solution clarification techniques and therefore would influence the light scattering measurements dramatically. Additionally, the low quantity of *t*-BuP_4 in the final copolymers (< 0.2 wt %) should not influence the physical properties of the material.[29]

Scheme 2. Presumed Side Reactions Leading to the Linear Diblock Copolymer Byproducts for the gPE Series (Table 1)

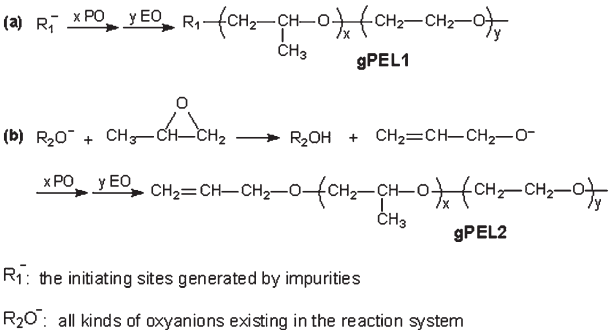

The composition of the side chains, shown in Table 1 as the weight fraction of PPO (f_{PO}), is calculated by the integral of the signals assigned to the methyl protons (δ = 0.8−1.4) and methylene/methine protons (δ = 3.2−4.0). By using the same characteristic peaks, we are also able to confirm that both gPE1L1 and gPE1L2 are composed of PPO and PEO; namely, they are both diblock copolymers. Moreover, traces of unsaturated C=C bond peaks (δ = 5.1−5.3) are found in the ^{1}H NMR spectrum of gPE1L2, indicating that the mechanism for the formation of this diblock copolymer must involve chain transfer to PO monomer.[35−38] The presumed side reactions resulting in the two linear copolymer byproducts are depicted in Scheme 2.

It has to be noted that this conclusion should only be reasonable for gPE series. For gEP1, the linear polymer byproduct with the lower molecular weight should be PPO homopolymer since PO is the second monomer added during the polymerization process. This is also evidenced by the fact that the peaks of the two byproducts are well separated in the SEC trace of gEP1 crude product (not shown). For gPE series, f_{PO} are close to the theoretical values ($f_{PO,theo}$, Table 1). However, f_{PO} of gEP1 is much lower than the theoretical value. This is because during the synthesis of gEP1 EO does not undergo the side reaction as PO (and as is the case for gPE1L2). Therefore, more EO is incorporated in the particular brush copolymer, yielding a lower f_{PO}.

Figure 4 shows the SEC traces for all the purified core−shell brush copolymers. Only gPE3 presents a symmetric SEC peak with the lowest polydispersity (M_w/M_n = 1.08, Table 1), while other products all present tailings in SEC peaks and relatively higher polydispersities (M_w/M_n > 1.10). It seems that the higher overall molecular weight and/or higher PEO content are the reasons for the tailing, since sorption of the copolymer on the styragel SEC columns might be taking place in this case.[40]

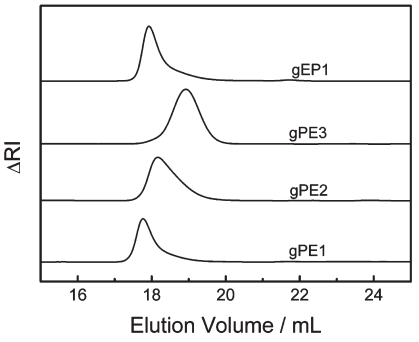

Figure 4. SEC traces of all purified core−shell brush copolymers (Table 1).

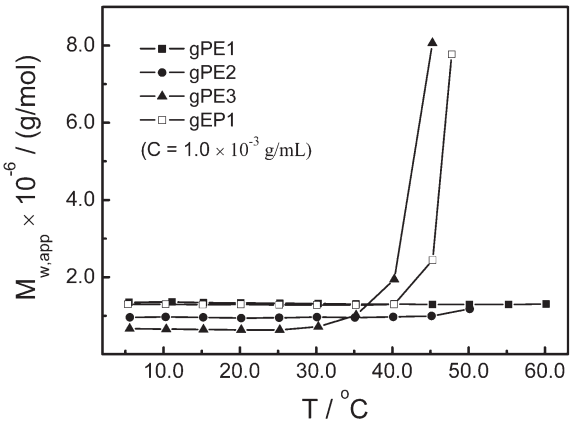

Figure 5. Temperature dependence of apparent weight-average molecular weight ($M_{w,app}$) of the core−shell brush copolymers in dilute aqueous solutions, where the polymer concentration is 1.0×10^{-3} g/mL.

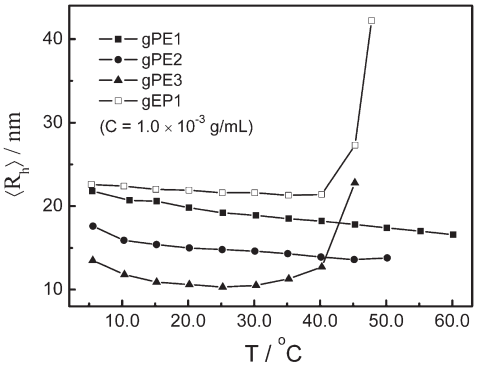

Figure 6. Temperature dependence of the average hydrodynamic radius ($\langle R_h \rangle$) of the core−shell brush copolymers in dilute aqueous solutions, where the polymer concentration is 1.0×10^{-3} g/mL.

The weight fraction of the oxyalkylene monomers incorporated in the brush copolymer during the graft polymerization (f_g, Table 1) is estimated using the peak areas in the SEC trace of each crude product. The molecular weight ($M_{w,cal}$, Table 1) of each brush copolymer in the crude product is roughly calculated by f_g and the known molecular weight of the backbone. The absolute molecular weights ($M_{w,LS}$, Table 1) of the fractionated brush copolymers are obtained from the SLS measurements (Zimm plots) in aqueous solution at 25 °C, with the concentration ranging from 4.0×10^{-4} to 1.0×10^{-3} g/mL. It can be seen in Table 1 that $M_{w,LS}$ is systematically larger than $M_{w,cal}$. Except for the inherent errors in these two methods for the calculation of molecular weights, the most important reason for the discrepancy is that a certain amount of the brush copolymer with relatively lower molecular weight is removed during the fractionation. Thus, a product with higher molecular weight is isolated ($M_{w,cal}$ was calculated by the peak areas in the SEC trace of the crude product, while $M_{w,LS}$ was determined for the fractionated pure brush copolymers).

The molecular weight of the side chains ($M_{w,arm}$, Table 1) is calculated by $M_{w,LS}$ and the molecular weight of the backbone, assuming that every repeat unit in the backbone is grafted with a side chain. Compared with the theoretical molecular weight of the side chain ($M_{arm,theo}$, Table 1), which is calculated by the feed ratio of the reagents for the graft polymerization, $M_{w,arm}$ is much lower, mostly due to the consumption of the monomers in the formation of linear copolymer byproducts. Judging from f_g, the polymerization for gPE2 gives the lowest yield in the brush copolymer. Our explanation is that gPE2 has the highest theoretical molecular weight of PPO (calculated from $M_{arm,theo}$ and $f_{PO,theo}$, Table 1), and the effect of the limiting molecular weight, ascribed to the chain transfer to PO monomer,[35] is more significant compared with other cases.

At present, it is still difficult for us to calculate quantitatively the grafting density, namely, the percentage of PhOH groups in the backbone grafted with side chains. This is also because (a) it is impossible to determine the amount of t-BuP_4 that participates in the deprotonation of the phenolic groups in the backbone in the first place and (b) PhOH groups, which are not deprotonated by t-BuP_4, might also generate initiating sites because of the overall protonation−deprotonation equilibrium during the polymerization, but the number of these PhOH groups is also impossible to be estimated.[16,29] Nevertheless, because of the high ratio of [t-BuP_4]/[PhOH] (0.9) used for the polymerization and reason b proposed above, the grafting density should be high for the copolymers prepared.

Thermoresponsive Behavior of the Core−Shell Brush Copolymers in Dilute Aqueous Solutions. The solutions used for LS measurements were prepared by dissolving each sample directly in water at 4 °C. This low temperature was used because for the samples with relatively higher PPO content (gPE2 and gPE3), complete dissolution cannot be reached at room temperature, which is evidenced by LS data (not shown). The concentration of each sample for the LS study in the heating process was fixed at 1.0×10^{-3} g/mL, which is a relatively high concentration for LS measurements, to ensure that the different aggregation behavior at various temperatures can be observed.

Figure 5 and 6 show the temperature dependence of apparent weight-average molecular weight ($M_{w,app}$) and average hydrodynamic radius ($\langle R_h \rangle$) for the core−shell brush copolymers, respectively. The aggregation temperature (T_{agg}) is defined as the temperature at which $M_{w,app}$ and $\langle R_h \rangle$ start to increase. In gPE series, gPE1, with the lowest f_{PO} (32.5%), does not aggregate but stays as dispersed unimers even at 60 °C. T_{agg} for gPE2 (f_{PO} = 59.2%) is ~50 °C, while for gPE3 (f_{PO} = 76.6%) is ~30 °C. It is obvious that for the gPE series the aggregation is facilitated by a higher PPO content in the copolymer. A constant and slight decrease of $\langle R_h \rangle$ can be observed for every gPE sample throughout the heating process (for sample gPE1) or in the lower temperature range before the aggregation takes place (for samples gPE2 and gPE3) (see also Figure 7). This should be attributed to the temperature-induced contraction and/or the intramolecular association of the PPO chains. This is because the hydrophobic attraction between PPO side chains increases as temperature increases. However, because of the excluded volume

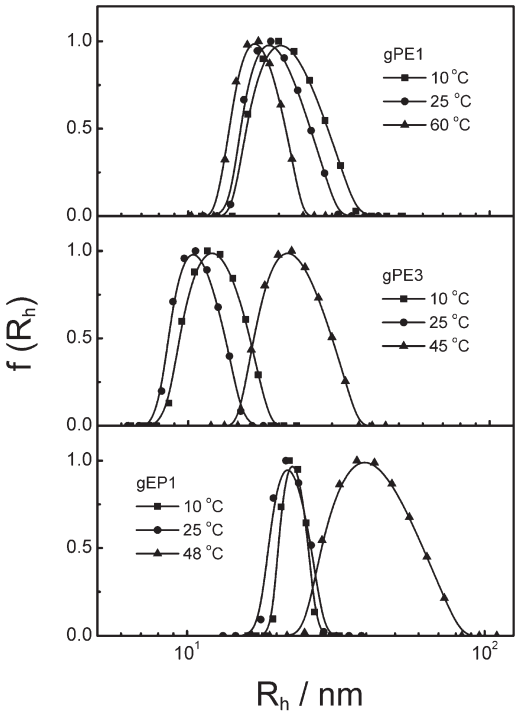

Figure 7. Temperature dependence of the hydrodynamic radius distribution ($f(R_h)$) at the scattering angle of 20° for the core−shell brush copolymers in dilute aqueous solutions, where the polymer concentration is 1.0×10^{-3} g/mL.

interactions and the inflexibility of the backbone, the chains only contract to a certain degree.[1,2,41,42]

For gEP1, further increase of the temperature leads to the intermolecular association of PPO side chains, which aggregate at ~45 °C. Noting that the PPO content of gEP1 is only 15.1% (Table 1), this is good evidence that the aggregation is favored by this inverse macromolecular structure. Comparing gEP1 with gPE3, we can see that the aggregation is more pronounced for gEP1 as the increase in both $M_{w,app}$ and $\langle R_h \rangle$ is faster. This can also be an evidence for the more favored aggregation, since it is much easier for PPO chains located at the periphery of the brush copolymer to contact and aggregate intermolecularly. The decrease of $\langle R_h \rangle$ for gEP1 before the aggregation is not so obvious compared to gPE series (see also Figure 7). Besides the lower content of PPO, the fact that PPO is not connected to the hydrophobic backbone may also be an important factor.

Compared with the linear copolymers composed of PPO and PEO,[17−19,43] it seems to be easier for these core−shell brush copolymers to undergo macroscopic phase separation than nanoscopic aggregation. This is probably because it is difficult for the core−shell brushlike macromolecular structure to form stable nanoscopic or microscopic suspended aggregates.

The thermoresponsive behavior of these core−shell brush copolymers was also investigated by fluorescence spectroscopy using pyrene as the probe. Figure 8 gives the temperature dependence of the intensity ratios, I_1/I_3 and I_e/I_m, in the pyrene fluorescence emission spectrum for gPE1 solution at the same concentration used for LS study ($C = 1.0 \times 10^{-3}$ g/mL). Unlike the case of the linear block copolymers,[43] I_1/I_3 starts with a much lower value (< 1.50) at the lowest temperature (also observed for other gPE samples) and decreases gradually as temperature rises. This indicates that even at low temperature the PPO chains, densely grafted on the backbone, are not completely solvated, and probably

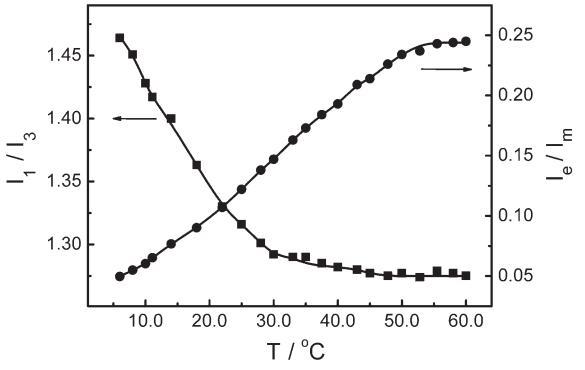

Figure 8. Plots of the intensity ratios (I_1/I_3 and I_e/I_m) in the pyrene fluorescence emission spectrum as a function of temperature for aqueous solution of sample gPE1 (Table 1), where the polymer concentration is 1.0×10^{-3} g/mL.

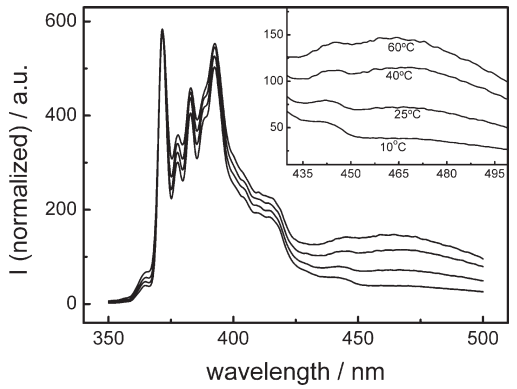

Figure 9. Fluorescence emission spectra of pyrene in water (2.7×10^{-7} M) in the presence of gPE1 (Table 1) at different temperatures, where the polymer concentration is 1.0×10^{-3} g/mL (the region corresponding to excimer fluorescence is shown in the inset).

some mildly dehydrated hydrophobic domains exist. The presence of a hydrophobic backbone must facilitate such a situation. When the temperature increases, the further dehydration and intramolecular contraction/association of PPO chains continue, and I_1/I_3 keeps decreasing until the minimum is reached at ~45 °C. The ratio of I_e/I_m goes up almost throughout the entire heating process (Figures 8 and 9), even after I_1/I_3 stays constant. This means that the contraction/association of the PPO chains continues and enhances the possibility for pyrene monomers to get close to each other, even when the polarity of the microenvironment stops changing.[43,44] This is also consistent with the constant decrease of $\langle R_h \rangle$ observed in LS measurements (Figure 6).

I_1/I_3 values for the samples that aggregate at high temperature (gPE2, gPE3, and gEP1) undergo two-stage decreases, assigned to the intramolecular chain contraction/association at lower temperature range and the intermolecular aggregation at higher temperature range. To make a better comparison, the temperature dependence of I_1/I_3 for gPE3 and gEP1 are shown in Figure 10. Throughout the heating process, gEP1 presents higher I_1/I_3 values compared with gPE3 and other gPE samples. The low content of PPO in gEP1 may be one reason. However, it should not be the most significant one here, considering that I_1/I_3 has still a relatively high value, even at high temperature after the intermolecular aggregation takes place. The best explanation should be the inverse molecular structure, which makes it more difficult for PPO chains to shrink or to form hydrophobic domains, either intramolecularly or intermolecularly.

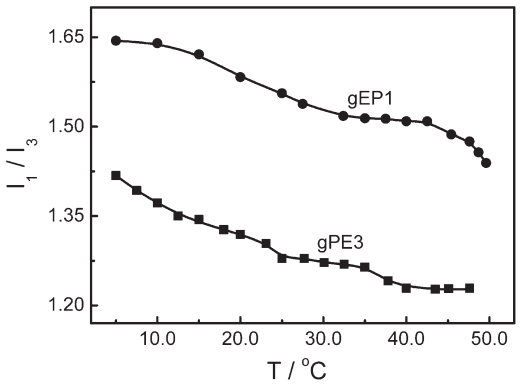

Figure 10. Plots of the intensity ratios (I_1/I_3) in the pyrene fluorescence emission spectrum as a function of temperature for aqueous solution of sample gPE3 and gEP1 (Table 1), where the polymer concentration is 1.0×10^{-3} g/mL.

The facts that the hydrophilic segments (PEO) of the side chains are tethered densely on the, probably rigidified, PHOS backbone, consequent chain stretching and the lowered chain mobility may be the most important reasons.

Conclusions

PHOS-*g*-(PPO-*b*-PEO) and PHOS-*g*-(PEO-*b*-PPO) core−shell brush copolymers have been successfully prepared. The diblock side chains are grafted by the "grafting from" technique via sequential metal-free anionic polymerization of PO and EO monomers, using the multifunctional initiating system generated by *t*-BuP_4 and the phenolic hydroxyl groups on the PHOS backbone. Two kinds of linear polymer byproducts are found in every crude product, which are attributed to different side reactions including the chain transfer to PO monomer. The brush copolymers could be easily purified by fractionation.

These core−shell brush copolymers presented thermoresponsive behavior in dilute aqueous solutions, which is quite different from that of the linear block copolymers comprised of PPO and PEO blocks. The fluorescence intensity ratio (I_1/I_3) reflects that, for the gPE series, PPO chains are not completely solvated even at 5 °C because they are densely grafted on the hydrophobic backbone. Both intramolecular chain contraction/association and intermolecular aggregation can be observed in the step-by-step heating process. It appears to be much easier for gEP to undergo intermolecular aggregation, compared to the gPE series, but compact hydrophobic domains do not exist in gEP unimers or aggregates.

Acknowledgment. J.Z. thanks the China Scholarship Council for offering the scholarship to work in TPCI-NHRF, Greece.

References and Notes

(1) Zhang, M.; Müller, A. H. E. *J. Polym. Sci., Part A: Polym. Chem.* **2005**, *43*, 3461–3481.
(2) Advincula, R. C., Brittain, W. J., Caster, K. C., Rühe, J., Eds.; *Polymer Brushes*; Wiley-VCH: Weinheim, 2004.
(3) Oliveira, C. M. F.; Lucas, E. F. *Polym. Bull.* **1990**, *24*, 363–370.
(4) Djalali, R.; Hugenberg, N.; Fischer, K.; Schmidt, M. *Macromol. Rapid Commun.* **1999**, *20*, 444–449.
(5) Heroguez, V.; Gnanou, Y.; Fontanille, M. *Macromolecules* **1997**, *30*, 4791–4798.
(6) Tusbaki, K.; Ishizu, K. *Polymer* **2001**, *42*, 8387–8393.
(7) Cheng, G.; Böker, A.; Zhang, M.; Krausch, G.; Müller, A. H. E. *Macromolecules* **2001**, *34*, 6883–6888.
(8) Zhang, M.; Breiner, T.; Mori, H.; Müller, A. H. E. *Polymer* **2003**, *44*, 1449–1458.
(9) Börner, H. G.; Beers, K.; Matyjaszewski, K. *Macromolecules* **2001**, *34*, 4375–4383.
(10) Bowden, N. B.; Dankova, M.; Wiyatno, W.; Hawker, C. J.; Waymouth, R. M. *Macromolecules* **2002**, *35*, 9246–9248.
(11) Cheng, C.; Qi, K.; Khoshdel, E.; Wooley, K. L. *J. Am. Chem. Soc.* **2006**, *128*, 6808–6809.
(12) Cheng, C.; Khoshdel, E.; Wooley, K. L. *Macromolecules* **2007**, *40*, 2289–2292.
(13) Zhang, M.; Drechsler, M.; Müller, A. H. E. *Chem. Mater.* **2004**, *16*, 537–543.
(14) Zhang, M.; Estournès, C.; Bietsch, W.; Müller, A. H. E. *Adv. Funct. Mater.* **2004**, *14*, 871–882.
(15) Hadjichristidis, N.; Roovers, J. *J. Polym. Sci., Part B: Polym. Phys.* **1978**, *16*, 851–858.
(16) Se, K.; Miyawaki, K.; Hirahara, K.; Takano, A.; Fujimoto, T. *J. Polym. Sci., Part A: Polym. Chem.* **1998**, *36*, 3021–3034.
(17) Almgren, M.; Brown, W.; Hvidt, S. *Colloid Polym. Sci.* **1995**, *273*, 2–15.
(18) Booth, C.; Attwood, D. *Macromol. Rapid Commun.* **2000**, *21*, 501–527.
(19) Nakashima, K.; Bahadur, P. *Adv. Colloid Interface Sci.* **2006**, *123−126*, 75–96.
(20) Lucas, E. F.; Oliveira, C. M. F. *Polym. Bull.* **1995**, *34*, 649–654.
(21) Robinson, K. L.; de Paz-Báñez, M. V.; Wang, X. S.; Armes, S. P. *Macromolecules* **2001**, *34*, 5799–5805.
(22) Förster, S.; Krämer, E. *Macromolecules* **1999**, *32*, 2783–2785.
(23) (a) Pispas, S.; Hadjichristidis, N. *Langmuir* **2003**, *19*, 48–54. (b) Pispas, S. *J. Polym. Sci., Part A: Polym. Chem.* **2006**, *44*, 606–613.
(24) Toy, A. A.; Reinicke, S.; Müller, A. H. E. *Macromolecules* **2007**, *40*, 5241–5244.
(25) Esswein, B.; Steidl, N. M.; Möller, M. *Macromol. Rapid Commun.* **1996**, *17*, 143–148.
(26) Schlaad, H.; Kukula, H.; Rudloff, J.; Below, I. *Macromolecules* **2001**, *34*, 4302–4304.
(27) Rexin, O.; Mülhaupt, R. *J. Polym. Sci., Part A: Polym. Chem.* **2002**, *40*, 864–873.
(28) Groenewolt, M.; Brezesinski, T.; Schlaad, H.; Antonietti, M.; Groh, P. W.; Iván, B. *Adv. Mater.* **2005**, *17*, 1158–1162.
(29) Zhao, J.; Mountrichas, G.; Zhang, G.; Pispas, S. *Macromolecules* **2009**, *42*, 8661–8668.
(30) (a) Hadjichristidis, N.; Iatrou, H.; Pispas, S.; Pitsikalis, M. *J. Polym. Sci., Part A: Polym. Chem.* **2000**, *38*, 3211–3234. (b) Uhrig, D.; Mays, J. W. *J. Polym. Sci., Part A: Polym. Chem.* **2005**, *43*, 6179–6222.
(31) Mountrichas, G.; Mantzaridis, C.; Pispas, S. *Macromol. Rapid Commun.* **2006**, *27*, 289–294.
(32) Mountrichas, G.; Pispas, S. *Macromolecules* **2006**, *39*, 4767–4774.
(33) (a) Huglin, M. B., Ed.; *Light Scattering from Polymer Solutions*; Academic: New York, 1972. (b) Teraoka, I. *Polymer Solutions*; John Wiley & Sons: New York, 2002. (c) Berne, B. J.; Pecora, R. *Dynamic Light Scattering*; Plenum Press: New York, 1976. (d) Chu, B. *Laser Light Scattering*, 2nd ed.; Academic Press: New York, 1991.
(34) *Polymer Handbook*, 3rd ed.; Brandup, J., Immergut, E. H., Eds.; Wiley-Interscience: New York, 1989.
(35) Price, C. C.; Carmelite, D. D. *J. Am. Chem. Soc.* **1966**, *88*, 4039–4044.
(36) Simons, D. M.; Verbanc, J. J. *J. Polym. Sci.* **1960**, *44*, 303–311.
(37) Ezra, G.; Zilkha, A. *Eur. Polym. J.* **1970**, *6*, 1305–1311.
(38) Jannasch, P. *Polymer* **2000**, *41*, 6701–6707.
(39) Kashiwa, N.; Matsugi, T.; Kojoh, S.-I.; Kaneko, H.; Kawahara, N.; Matsuo, S.; Nobori, T.; Imuta, J.-I. *J. Polym. Sci., Part A: Polym. Chem.* **2003**, *41*, 3657–3666.
(40) Gauthier, M.; Tichagwa, L.; Downey, J. S.; Gao, S. *Macromolecules* **1996**, *29*, 519–527.
(41) Hu, T.; Wu, C. *Phys. Rev. Lett.* **1999**, *83*, 4105–4107.
(42) Hu, T.; Wu, C. *Macromolecules* **2001**, *34*, 6802–6805.
(43) Nivaggioli, T.; Alexandridis, P.; Hatton, T. A.; Yekata, A.; Winnik, M. A. *Langmuir* **1995**, *11*, 730–737.
(44) Yekta, A.; Duhamel, J.; Brochard, P.; Adiwidjaja, H.; Winnik, M. A. *Macromolecules* **1993**, *26*, 1829–1836.